HHS Public Access

Author manuscript

Nature. Author manuscript; available in PMC 2011 January 01.

Published in final edited form as:

Nature. 2010 July 15; 466(7304): 393–397. doi:10.1038/nature09252.

Structure of the Gating Ring from the Human High-conductance Ca^{2+}-gated K^+ Channel

Yunkun Wu[1,2], **Yi Yang**[1], **Sheng Ye**[3], and **Youxing Jiang**[1,2]

[1]Department of Physiology, University of Texas Southwestern Medical Center, Dallas, Texas 75390-9040

[2]Howard Hughes Medical Institute, University of Texas Southwestern Medical Center, Dallas, Texas 75390-9040

[3]Life Sciences Institute, Zhejiang University, Hangzhou, Zhejiang 310058, P.R. China

Abstract

High-conductance Ca^{2+}-gated K^+ (BK) channels are essential for many biological processes such as smooth muscle contraction and neurotransmitter release[1-4]. This group of channels can be activated synergistically by both voltage and intracellular Ca^{2+}, with the large C-terminal intracellular portion being responsible for Ca^{2+} sensing[5-13]. Here we present the crystal structure of the entire cytoplasmic region of the human BK channel in a Ca^{2+} free state. The structure reveals four intracellular subunits, each comprising two tandem RCK domains, assembled into a gating ring similar to that seen in the MthK channel[14] and likely representing its physiological assembly. Three Ca^{2+} binding sites including the Ca^{2+} bowl are mapped onto the structure based on mutagenesis data. The Ca^{2+} bowl, located within the second RCK domain, forms an EF-hand like motif and is strategically positioned close to the assembly interface between two subunits. The other two Ca^{2+} (or Mg^{2+}) binding sites, Asp367 and Glu374/Glu399, are located on the first RCK domain. The Asp367 site has high Ca^{2+} sensitivity and is positioned in the groove between the N- and C- terminal subdomains of RCK1, whereas the low affinity Mg^{2+}-binding Glu374/Glu399 site is positioned on the upper plateau of the gating ring and close to the membrane. Our structure also contains the linker connecting the transmembrane and intracellular domains, allowing us to dock a voltage-gated K^+ channel pore of known structure onto the gating ring with reasonable accuracy and generate a structural model for the full BK channel.

Address correspondence to: Youxing Jiang, Department of Physiology, UT Southwestern Medical Center, 5323 Harry Hines Blvd., Dallas, Texas 75390-9040, Tel. 214 645-6027; Fax. 214 645-6042; youxing.jiang@utsouthwestern.edu.

Supplementary Information is linked to the online version of the paper at http://www.nature.com/nature.

Author Contributions. Y.W performed sample preparation and structure determination. Y.Y performed protein expression and purification. S.Y performed model building and refinement. Y.W and Y.J. designed the research, analyzed data, and prepared the manuscript.

Author information. The atomic coordinates and structure factors have been deposited in the Protein Data Bank under accession number 3NAF. Reprints and permissions information is available at npg.nature.com/reprintsandpermissions. The authors declare no competing financial interests. Correspondence and requests for materials should be addressed to Y.J. (youxing.jiang@utsouthwestern.edu).

BK channels, also called MaxiK or Slo1, are a vital class of K^+ channels found throughout the animal kingdom and expressed in a variety of cell types[1-4]. Several unique biophysical properties, including a large conductance and a gating mechanism involving both voltage and intracellular Ca^{2+}, distinguish them from other K^+ channels. The S1-S4 transmembrane region of BK channels forms a voltage sensing domain (VSD) as in other voltage-gated K^+ channels, whereas the large C-terminal intracellular ligand binding part, accounting for two thirds of the full channel, is responsible for sensing Ca^{2+}([5-13]) as well as other intracellular stimuli[15]. The latter has been predicted to contain two RCK domains, first identified in an *E.coli* K^+ channel and conserved in the majority of prokaryotic ligand-gated K^+ channels[14,16] as well as in the bacterial K^+ uptake and efflux machinery (the KTN domain)[17,18]. While the first RCK domain of BK shares high sequence similarity with its prokaryotic counterparts, the less homologous second RCK domain is not as well defined. Even though the intracellular ligand gating properties of BK channels have been extensively studied, little is known about the structural details underlying their ligand gating mechanism beyond the proposed models based on MthK[16,19,20] and a recent low resolution structure from electron cryomicroscopy[21]. The structure of the intracellular ligand binding domain presented here therefore provides essential structural information to guide future studies aimed at understanding how these physiologically essential channels integrate multiple cellular stimuli to modulate membrane excitability.

A human BK (hslo1) intracellular domain construct starting from Arg329, located right after the pore lining inner helix, to the C-terminal end (Supplementary Fig. 1) was chosen for structural characterization. Additionally, an extra 32-amino acid sequence from a mutant transcription factor GCN4 leucine zipper (GCN4_LI) known to form a 4-helical coiled-coil domain was inserted before the N-terminus of the BK intracellular domain. The protein was also treated with Lambda protein phosphatase before crystallization. Both modifications proved essential to obtaining good quality crystals. The crystals, which were of space group *I*422 and contained one subunit per asymmetric unit, revealed four crystallographically related subunits assembled as a tetramer with the molecular 4-fold coinciding with the crystallographic tetrad. The final model was refined to 3.1 Å with R_{work} of 23.8 % and R_{free} of 28.9 % (Methods and Table I).

Despite low sequence identity and large differences in sequence length between BK channels and prokaryotic RCK-regulated K^+ channels, the intracellular portion of human BK contains two tandem RCK domains as predicted[14] and its structure is strikingly similar to that of its prokaryotic counterpart, the MthK channel (Fig. 1 and Supplementary Fig. 1 & 2). For comparative purposes, secondary structure elements of each BK RCK domain are labeled following the same nomenclature used for its prokaryotic counterparts (Supplementary Fig. 1).

Each RCK domain can be divided into three subdomains: an N-terminal Rossmann folded subdomain (from βA to βF) that forms the central core of the gating ring; the intermediate helix-crossover domain (αF-turn-αG) that interlocks the two RCK domains; and a C-terminal subdomain that interacts with its counterpart from a neighboring RCK domain within the same subunit (Fig. 1a&b and Supplementary Fig. 2). The two RCK domains form a bi-lobed architecture with extensive inter-RCK interactions at the helix cross-over and C-

terminal subdomain, reminiscent of the RCK homodimer in MthK (Fig. 1c&d). Interestingly the deep cleft between the two RCK domains of MthK as well as other prokaryotic RCK proteins is occupied in the BK channel mainly by residues from the extended loops between βD and αD of both RCKs (Fig. 1c). Whereas this wide open cleft allows for large conformational changes at the flexible interface at its base in MthK upon ligand binding, its absence in BK raises the question whether similar conformational changes also occur. Further studies are needed to address this issue.

Four BK intracellular subunits assemble as a gating ring of eight RCK domains. The Rossmann folded subdomains from eight RCKs form the central core of the gating ring while the C-terminal subdomains form four protruded knobs at its periphery (Fig. 2a). The inter-subunit interactions occur at the assembly interface formed by helices αD and αE from each RCK domains in a head-to-tail manner; that is, RCK1 contacts RCK2 from the neighboring subunit. The protein-protein contacts at the assembly interface are mainly hydrophobic, involving residues Ile441, Met442, Ile445 on αD and His468 on αE of RCK1 and residues Ile821, Leu822, Leu825 and Phe890 on the equivalent helices of RCK2 from the neighboring subunit (Fig. 2b and Supplementary Fig. 3). The three residues on αD that form the core of the assembly interface are conserved as hydrophobic in most RCK domains[14,16]. Interestingly, αEs from both BK RCK domains appear to be 3_{10} helices. Compared to MthK, the BK gating ring is more expanded, as expected for a protein of much larger size. The diagonal distance of the gating ring is about 82 Å, measured between the Cα atoms of Arg342 residues located at the outer rim of the ring (Fig. 2c). The BK gating ring also has a wide central hole with a width of about 20 Å, allowing ions to move freely between the ion conduction pore and the intracellular side. The crystals were obtained in the absence of Ca^{2+} and no bound divalent cations were observed in the structure. This led us to suggest that the BK gating ring structure shown here might represent a closed conformation.

While the BK intracellular domain is responsive to various chemical stimuli inside the cell, Ca^{2+} activation has so far been best characterized and will be the focus of the discussion here. Micromolar concentrations of Ca^{2+} can activate voltage-dependent gating of BK channels[4,22,23]. This high Ca^{2+} sensitivity can be partly attributed to a stretch of well-conserved aspartate residues within the second RCK domain, known as the Ca^{2+} bowl[6,7]. The Ca^{2+} bowl is located right after αE in the second RCK followed by a short helix (αEF), and is physically in close proximity to the assembly interface (Fig. 3a&b). Our structure was determined in the absence of Ca^{2+} and the stretch of acidic residues in the Ca^{2+} bowl does not form a well ordered structure. The short helix following the Ca^{2+} bowl is not seen on BK RCK1 and other RCK proteins, and was assigned as αEF since it is between αE and βF. Together with the Ca^{2+} bowl and αE, this helix forms a helix-loop-helix motif (αE-loop-αEF) very similar to Ca^{2+} binding EF-hand proteins such as Calmodulin[24,25] (Fig. 3c), despite αEF being much shorter than the exiting helix (F helix) of most EF-hand proteins. It is likely that the disordered Ca^{2+} bowl structure represents an apo state and becomes ordered upon Ca^{2+} binding as commonly seen in EF-hand proteins which are also rich in acidic residues at the Ca^{2+} binding loop[25]. The strategic location of the Ca^{2+} bowl besides the inter-subunit assembly interface led us to postulate that Ca^{2+} binding triggers conformational changes at the assembly interface, changing the size of the gating ring and leading to channel activation.

In addition to the Ca^{2+} bowl, recent studies have also identified at least two other independent Ca^{2+} binding sites within the first RCK domain[8-12]. One such site also has high Ca^{2+} sensitivity and involves an acidic residue, Asp367, located on the loop between αA and βB. In context of the gating ring, this site is positioned in the groove between the N- and C-terminal subdomains of RCK1, exposed to the open space between the membrane and the peripheral C-terminal subdomain (Fig. 3a). Figure 3d shows the chemical environment surrounding Asp367, comprising the side chains of His365, Met513, and Glu535. His365 has been shown to be involved in pH activation of BK and was proposed to interact electrostatically with Asp367 upon protonation[26], mimicking the effect of Ca^{2+}. The location of Met513 at this site explains the profound effect on Ca^{2+} sensitivity observed upon mutation[9]. Even though the side chain of Met513 may not directly bind Ca^{2+}, it may play a key role in maintaining the local structural integrity of the Ca^{2+} binding site. The chemistry of the Asp367 ion binding site with a limited number of ligands does not seem suitable for high affinity Ca^{2+} binding. It is likely that residues from other parts of the channel may participate in Ca^{2+} binding. One possibility is residue Glu535 on the C-terminal subdomain of RCK1 whose side chain seems to be perfectly positioned to chelate Ca^{2+} together with Asp367, and may well be involved in Ca^{2+} binding, a hypothesis that warrants further investigation through mutagenesis.

The second Ca^{2+} binding site on RCK1 has lower affinity and has been suggested to be physiologically regulated by Mg^{2+}([10,11,27]). This low affinity site formed by Glu374 and Glu399 located on two neighboring β strands, βB and βC, respectively (Fig. 3e), is very close to the linker between the gating ring and the channel pore. The hydroxyl group of Ser337 on the linker is oriented towards the ion binding site and could also serve as a ligand for Ca^{2+} (or Mg^{2+}). This site is positioned on the upper plateau of the gating ring near the membrane surface (Fig. 3a), suggesting that residues from the intracellular-facing part of the membrane spanning channel may participate in forming ion binding sites. Indeed, a recent study has pointed to an acidic residue from the large S0-S1 loop being important for Mg^{2+} binding[27].

The protein construct used in our structural study contains the linker region thought to directly connect the gating ring to the pore lining inner helices of the transmembrane pore. This linker has an extended strand-like structure pointing towards the center of the gating ring (Fig. 2a & 4) and does not seem to form any specific non-covalent interactions with other parts of the protein. A stretched conformation likely allows the four linkers of a functional BK tetramer to more effectively couple gating ring conformational changes to pore opening and closing. Indeed, insertion and deletion mutations at the linker region have a profound effect on BK channel gating[28].

The formation of a 4-helical coiled-coil by the attached GCN4_LI in effect mimics the pore-lining inner helices in constraining the linker. We believe it does not adversely affect the linker structure as we observe a similar orientation and extended strand like structure of the linker connecting the pore and transmembrane ligand binding domain in a recent structure of a bacterial K^+ channel from *Geobacter sulfurreducens*, which contains 2-tandem RCK domains as in BK channels, solved recently by our group (unpublished results). Taken

together, these data provide plausible evidence suggesting that the linker structure seen in the BK gating ring is physiologically relevant.

The presence of the linker between the BK gating ring and its channel pore allowed us to generate a full channel model by docking a voltage gated K^+ channel onto the gating ring (Supplementary Fig. 4). The S1-S6 portion of the Kv1.2 structure[29] was used as an approximate model for the BK transmembrane pore and was positioned onto the BK gating ring assembly with its C-terminal end of the S6 inner helix right at the N-terminus of the BK linker. Even though specific architectural features of BK and Kv channels may be different, we nevertheless believe this full channel model provides useful information about the relative positioning/orientation of the BK ligand binding domain with respect to the pore.

A 3 Å monomeric crystal structure of the human BK intracellular domain along with a terameric gating ring model based upon the 6 Å cytoplasmic subunit structure of the chicken Slo2 channel, a Na^+-activated BK homolog, was published immediately preceding this paper by the Mackinnon group[30]. The overall architecture of the individual subunits and the deduced gating ring model match very well with the structure of our tetrameric gating ring assembly. Moreover, in the presence of 50 mM Ca^{2+}, the authors suggest their structures represent the ligand-bound, open conformation compared to our ligand-free structure. Taken together, these related studies provide the first glimpse of two possible gating-ring conformations of BK channels.

Methods Summary

The intracellular fragment of the human *Slo1* gene was subcloned into the pFastBac-HTa vector and expressed in SF9 insect cells using a baculovirus system. The construct contains an N-terminal His-tag, TEV protease cleavage site and an extra 32-amino acid stretch of sequence RMKQIEDKLEEILSKLYHIENELARIKKLLGE from the mutant transcription factor GCN4 leucine zipper (GCN4_LI) immediately before the N-terminus of the BK intracellular domain. Expressed protein was first purified on Co^{2+} affinity resin followed by overnight TEV cleavage at 4 °C to remove the His-tag. Protein was concentrated and then treated with Lambda protein phosphatase before further purification on a gel filtration column. Purified protein was concentrated to about 7 mg/ml and crystallized at 4 °C using the sitting drop vapor diffusion method by mixing equal volumes of concentrated protein and well solution containing 3.5 M sodium formate and 0.1 M Tris.HCl, pH 8.5. The crystals were of space group *I*422 with cell dimensions of a=b=134.1 Å, c=231.6 Å, α=β=γ=90°, and contained one subunit per asymmetric unit. The structure was determined by single wavelength anomalous dispersion (SAD) using selenomethionine substituted protein crystals. Model building was aided by the Se sites and conserved structure features of RCK domains. The final model was refined to 3.1 Å with R_{work} of 23.8% and R_{free} of 28.9%, and contained residues 330 to 616, 684 to 833, and 872 to 1059. The density for the N-terminal GCN4_LI coiled-coil is weak and is not modeled in the final structure.

Supplementary Material

Refer to Web version on PubMed Central for supplementary material.

Acknowledgments

We thank A. Alam and M. Derebe for manuscript preparation; A. Pico for discussion in the early stages of this study; and X. Zhang for help in structure determination. Use of the Advanced Photon Source (APS) was supported by the US Department of Energy, Office of Energy Research. We thank the beamline (23ID and 19ID) staff for assistance in data collection. This work was supported by Howard Hughes Medical Institute and by grants from the NIH/NIGMS (RO1 GM071621) and Welch Foundation.

References

1. Kaczorowski GJ, Knaus HG, Leonard RJ, McManus OB, Garcia ML. High-conductance calcium-activated potassium channels; structure, pharmacology, and function. J Bioenerg Biomembr. 1996; 28(3):255–267. [PubMed: 8807400]
2. Latorre R, Oberhauser A, Labarca P, Alvarez O. Varieties of calcium-activated potassium channels. Annu Rev Physiol. 1989; 51:385–399. [PubMed: 2653189]
3. Cui J, Yang H, Lee US. Molecular mechanisms of BK channel activation. Cell Mol Life Sci. 2008
4. Magleby KL. Gating mechanism of BK (Slo1) channels: so near, yet so far. J Gen Physiol. 2003; 121(2):81–96. [PubMed: 12566537]
5. Wei A, Solaro C, Lingle C, Salkoff L. Calcium sensitivity of BK-type KCa channels determined by a separable domain. Neuron. 1994; 13(3):671–681. [PubMed: 7917297]
6. Schreiber M, Salkoff L. A novel calcium-sensing domain in the BK channel. Biophys J. 1997; 73(3):1355–1363. [PubMed: 9284303]
7. Bao L, Kaldany C, Holmstrand EC, Cox DH. Mapping the BKCa channel's “Ca2+ bowl”: side-chains essential for Ca2+ sensing. J Gen Physiol. 2004; 123(5):475–489. [PubMed: 15111643]
8. Zhang X, Solaro CR, Lingle CJ. Allosteric regulation of BK channel gating by Ca(2+) and Mg(2+) through a nonselective, low affinity divalent cation site. J Gen Physiol. 2001; 118(5):607–636. [PubMed: 11696615]
9. Bao L, Rapin AM, Holmstrand EC, Cox DH. Elimination of the BK(Ca) channel's high-affinity Ca(2+) sensitivity. J Gen Physiol. 2002; 120(2):173–189. [PubMed: 12149279]
10. Xia XM, Zeng X, Lingle CJ. Multiple regulatory sites in large-conductance calcium-activated potassium channels. Nature. 2002; 418(6900):880–884. [PubMed: 12192411]
11. Shi J, et al. Mechanism of magnesium activation of calcium-activated potassium channels. Nature. 2002; 418(6900):876–880. [PubMed: 12192410]
12. Zeng XH, Xia XM, Lingle CJ. Divalent cation sensitivity of BK channel activation supports the existence of three distinct binding sites. J Gen Physiol. 2005; 125(3):273–286. [PubMed: 15738049]
13. Xia XM, Zhang X, Lingle CJ. Ligand-dependent activation of Slo family channels is defined by interchangeable cytosolic domains. J Neurosci. 2004; 24(24):5585–5591. [PubMed: 15201331]
14. Jiang Y, et al. Crystal structure and mechanism of a calcium-gated potassium channel. Nature. 2002; 417(6888):515–522. [PubMed: 12037559]
15. Hou S, Heinemann SH, Hoshi T. Modulation of BKCa channel gating by endogenous signaling molecules. Physiology (Bethesda). 2009; 24:26–35. [PubMed: 19196649]
16. Jiang Y, Pico A, Cadene M, Chait BT, MacKinnon R. Structure of the RCK domain from the E. coli K+ channel and demonstration of its presence in the human BK channel. Neuron. 2001; 29(3): 593–601. [PubMed: 11301020]
17. Albright RA, Ibar JL, Kim CU, Gruner SM, Morais-Cabral JH. The RCK domain of the KtrAB K+ transporter: multiple conformations of an octameric ring. Cell. 2006; 126(6):1147–1159. [PubMed: 16990138]
18. Roosild TP, Miller S, Booth IR, Choe S. A mechanism of regulating transmembrane potassium flux through a ligand-mediated conformational switch. Cell. 2002; 109(6):781–791. [PubMed: 12086676]
19. Kim HJ, Lim HH, Rho SH, Eom SH, Park CS. Hydrophobic interface between two regulators of K + conductance domains critical for calcium-dependent activation of large conductance Ca2+-activated K+ channels. J Biol Chem. 2006; 281(50):38573–38581. [PubMed: 17040919]

20. Yusifov T, Savalli N, Gandhi CS, Ottolia M, Olcese R. The RCK2 domain of the human BKCa channel is a calcium sensor. Proc Natl Acad Sci U S A. 2008; 105(1):376–381. [PubMed: 18162557]
21. Wang L, Sigworth FJ. Structure of the BK potassium channel in a lipid membrane from electron cryomicroscopy. Nature. 2009; 461(7261):292–295. [PubMed: 19718020]
22. Horrigan FT, Aldrich RW. Coupling between voltage sensor activation, Ca2+ binding and channel opening in large conductance (BK) potassium channels. J Gen Physiol. 2002; 120(3):267–305. [PubMed: 12198087]
23. Lingle CJ. Setting the stage for molecular dissection of the regulatory components of BK channels. J Gen Physiol. 2002; 120(3):261–265. [PubMed: 12198086]
24. Falke JJ, Drake SK, Hazard AL, Peersen OB. Molecular tuning of ion binding to calcium signaling proteins. Q Rev Biophys. 1994; 27(3):219–290. [PubMed: 7899550]
25. Gifford JL, Walsh MP, Vogel HJ. Structures and metal-ion-binding properties of the Ca2+-binding helix-loop-helix EF-hand motifs. Biochem J. 2007; 405(2):199–221. [PubMed: 17590154]
26. Hou S, Xu R, Heinemann SH, Hoshi T. Reciprocal regulation of the Ca2+ and H+ sensitivity in the SLO1 BK channel conferred by the RCK1 domain. Nat Struct Mol Biol. 2008; 15(4):403–410. [PubMed: 18345016]
27. Yang H, et al. Activation of Slo1 BK channels by Mg2+ coordinated between the voltage sensor and RCK1 domains. Nat Struct Mol Biol. 2008; 15(11):1152–1159. [PubMed: 18931675]
28. Niu X, Qian X, Magleby KL. Linker-gating ring complex as passive spring and Ca(2+)-dependent machine for a voltage- and Ca(2+)-activated potassium channel. Neuron. 2004; 42(5):745–756. [PubMed: 15182715]
29. Long SB, Tao X, Campbell EB, MacKinnon R. Atomic structure of a voltage-dependent K+ channel in a lipid membrane-like environment. Nature. 2007; 450(7168):376–382. [PubMed: 18004376]
30. Yuan P, Leonetti MD, Pico AR, Hsiung Y, Mackinnon R. Structure of the Human BK Channel Ca2+-Activation Apparatus at 3.0 A Resolution. Science. Published Online May 27, 2010.

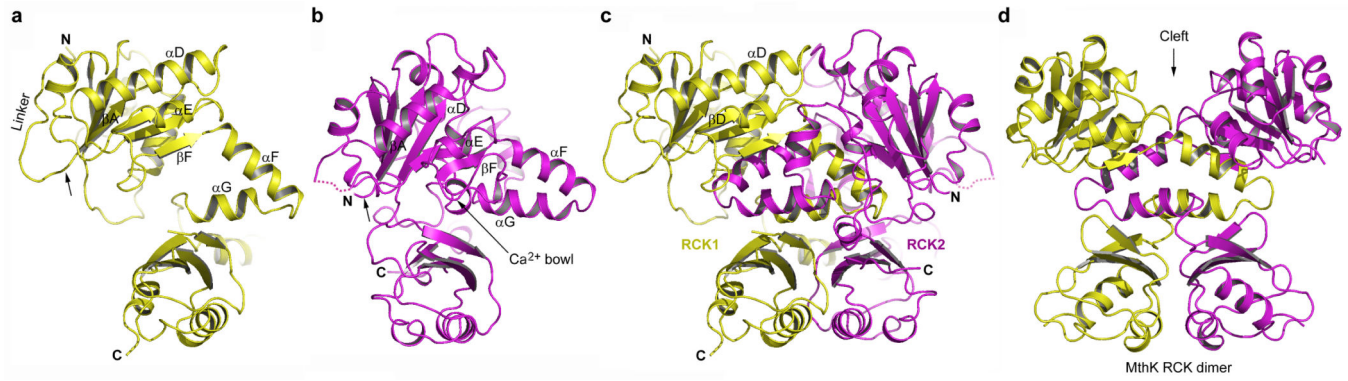

Figure 1.

The BK intracellular subunit contains two RCK domains. The structure of the individual RCK domain is shown in **a**, RCK1 (yellow) and **b**,RCK2 (magenta). Only selected secondary structural elements are labeled for clarity. The arrow indicates the starting point of each RCK. and the linker connects RCK1 to the channel pore. The disordered loop between αD and βE on RCK2 is drawn as dotted line. **c**, The BK intracellular subunit is comprised of RCK1 and RCK2, and the orientation of RCK1 shown in the subunit assembly is the same as in (**a**). The long loop connecting the C-terminus of RCK1 and N-terminus of RCK2 is disordered. **d**, The structure of the RCK homodimer in MthK is shown with RCK domains colored yellow and magenta, respectively. Stereo diagrams of BK domain structures are shown in Supplementary Figures.

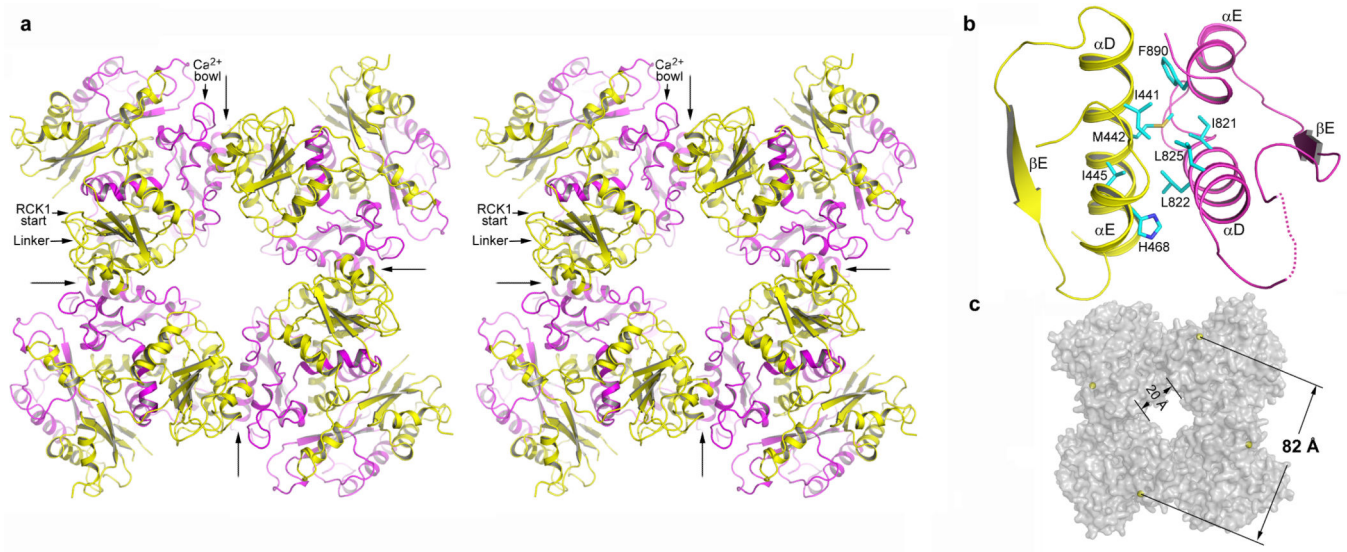

Figure 2.

Four BK intracellular subunits assemble into a gating ring. **a**, Stereo diagram of the gating ring structure viewed down the 4-fold axis from the extracellular side. Four long arrows indicate the position of inter-subunit assembly interfaces and define the boundary of each subunit. RCK1 and RCK2 in each subunit are colored yellow and magenta, respectively. The linker between RCK1 and the channel pore, the starting point of RCK1, and the position of the Ca^{2+} bowl are labeled on one subunit (upper left corner). **b**, An enlarged view of the assembly interface formed by helices αD and αE from both RCK1 (yellow) and RCK2 (magenta). The side chains of those hydrophobic residues important for protein-protein contacts are also shown. The disordered loop between αD and βE is drawn as a dotted line. **c**, Overall shape of the BK gating ring in surface representation. Yellow spheres represent the Cα atoms from Arg342s used to define the diagonal length of the gating ring.

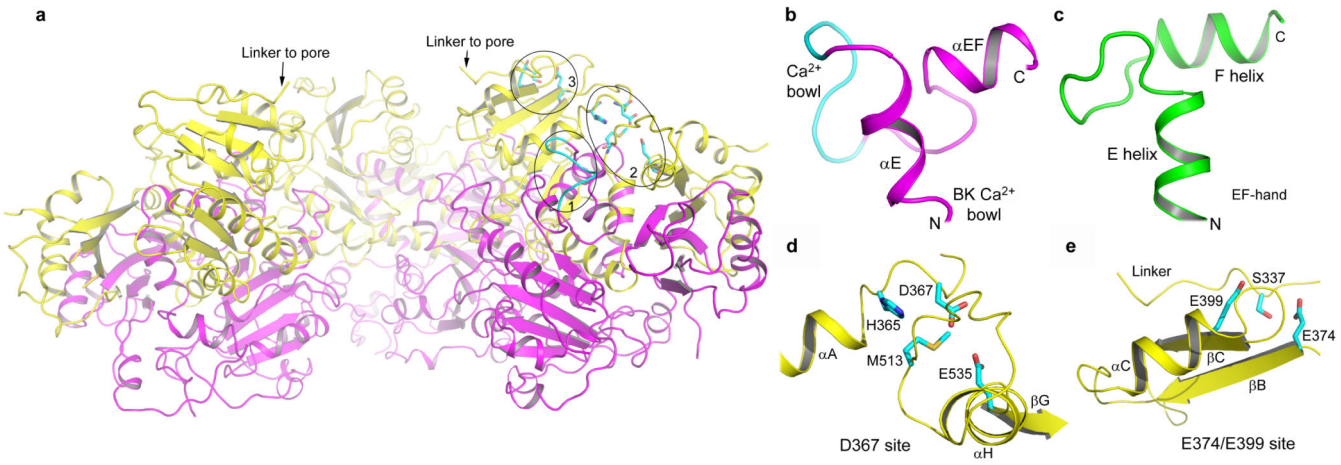

Figure 3.

Ca^{2+} binding sites in the BK intracellular subunit. **a**, A side view of the BK gating ring with the top surface facing the membrane. The front subunit is removed for clarity. The circled positions represent the three Ca^{2+} binding sites on one subunit, and are labeled 1 for the Ca^{2+} bowl, 2 for the Asp367 site and 3 for the Glu374/Glu399 site. **b**, αE, the Ca^{2+} bowl, and αEF form an EF-hand like motif. The structure of the Ca^{2+} bowl (cyan loop) is disordered in the absence of Ca^{2+}. **c**, The EF-hand structure of a Ca^{2+} binding protein (a human Calmodulin molecule with PDB code 1CLL). **d** and **e**, Structural details of the Asp367 and E374/E399 Ca^{2+} binding sites, respectively.

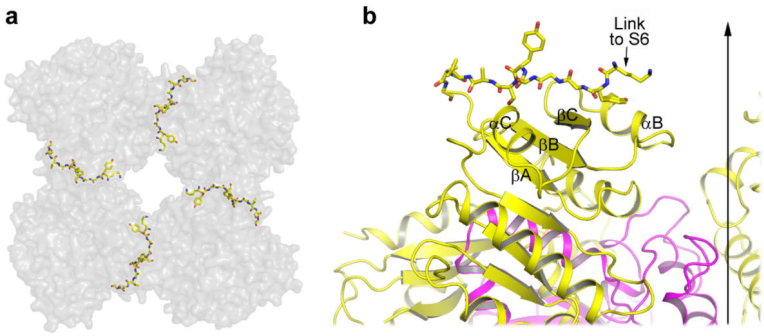

Figure 4.

Structure of the linker between the gating ring and the channel pore. **a**, Top view of the four linkers (shown in ball and stick representation) between the gating ring (grey surface representation) and the channel pore. **b**, An enlarged side view of the extended linker (ball and stick) on top of RCK1 (yellow). The vertical arrow indicates the central 4-fold axis of the gating ring.